Theoretical calculation of x-ray magnetic circular dichroism spectra for Gd/Cu multilayers at the Cu K edge

2005 J. Phys.: Condens. Matter 17 5785

(http://iopscience.iop.org/0953-8984/17/37/014)

INSTITUTE OF PHYSICS PUBLISHING JOURNAL OF PHYSICS: CONDENSED MATTER

J. Phys.: Condens. Matter **17** (2005) 5785–5794 doi:10.1088/0953-8984/17/37/014

Theoretical calculation of x-ray magnetic circular dichroism spectra for Gd/Cu multilayers at the Cu K edge

J Minár[1,3], A Perlov[1], H Ebert[1] and H Hashizume[2,4]

[1] Department Chemie, Physikalische Chemie, Universität München, Butenandstraße 5-13, Haus E-2.037, D-81337 München, Germany
[2] Research and Education Center for Materials Science, Nara Institute of Science and Technology, Takayama, Ikoma 630-0192, Japan

E-mail: Jan.Minar@cup.uni-muenchen.de

Received 21 March 2005, in final form 17 August 2005
Published 2 September 2005
Online at stacks.iop.org/JPhysCM/17/5785

Abstract

To explain the remarkable oscillations observed in the x-ray magnetic circular dichroic absorption spectra from Gd/Cu multilayers at the Cu K edge, *ab initio* calculations have been made using the fully relativistic Korringa–Kohn–Rostoker formalism including the spin–orbit coupling. The result reproduces well the oscillatory profiles in the near-edge region, but the peaks and valleys do not correspond to those in the difference density of states $n_\uparrow - n_\downarrow$ for the unoccupied Cu 4p band above the Fermi level. We find small spin and orbital moments on the interfacial Cu sites, which decay towards the core of the Cu layer. Surprisingly, neither the spin nor the orbital moments die out on the Cu sites four atomic layers away from the Co interface. This extended polarization is ascribed to the hybridization of the Cu 4p and the Gd 5d states. The accuracy of the calculation is supported by the near-bulk spin and orbital moments found on the Gd sites away from the interface.

1. Introduction

The magnetic polarization of nonmagnetic spacer metals is a key factor to improve the understanding of the physical properties of exchange-coupled magnetic/nonmagnetic multilayers and sandwiches, which find applications in high-density disks, magnetic random access memories, and other spintronic devices [1]. Among the various exchange-coupled metal systems reported [2, 3], Co/Cu is a classical system, which is the most extensively studied both theoretically and experimentally [4]. In this system, nearly free electrons in the Cu layers

[3] Author to whom any correspondence should be addressed.
[4] Present address: Photon Factory, KEK, Oho, Tsukuba 305-0801, Japan.

become spin polarized by magnetic interaction with Co atoms at the interface. The polarization propagates across the Cu layer and interacts with another Co layer, thereby giving rise to an interlayer coupling between the Co moments [5, 6]. The confined electrons in the Cu layer have a minority-spin character and form quantum-well states with discrete densities of states near the Fermi level, as evidenced by photoemission measurements [6–10, 3]. The minority character of delocalized Cu electrons was confirmed in x-ray magnetic circular dichroism (XMCD) measurements [11, 12, 4], while a multiple-scattering calculation showed that the Cu dichroism is primarily due to the spin-dependent scattering of photoelectrons emitted from x-ray absorbing Cu atoms by nearby Co atoms [4]. The magnetic moments induced on the Cu sites make marginal contributions to the observed Cu dichroism [4]. The spin-density distribution across the Cu layer was probed in a recent resonant x-ray magnetic scattering experiment, which reveals a large local spin density at the Co/Cu interface, decaying in an oscillatory fashion towards the core of the Cu layer [13]. As to the oscillatory coupling as a function of the spacer thickness [14], the long and short oscillation periods (Λ) observed in Co/Cu [15, 16] and other multilayers of 3d ferromagnets and nonmagnetic metallic spacers [17–22] are amply explained by the quantum-interference model of the interlayer magnetic coupling in terms of the spanning vectors ($\mathbf{q}$) connecting the extremal points on the spacer Fermi surface in the out-of-plane direction, i.e., $\Lambda = 2\pi/|\mathbf{q}|$ [5, 6]. This model assumes spin-dependent reflections of nearly free electrons in nonmagnetic spacer layers at the interface with reflection coefficients determined by the matching of the spacer band structure and the exchange-split band structures of ferromagnetic metals [5].

In comparison, much less is known about the magnetic polarization of spacer metal in rare-earth multilayers and sandwiches. Takanashi *et al* [23] reports monotonically decreasing exchange couplings between Gd and Co in Gd/Cu/Co and Gd/Y/Co multilayers with increasing Cu and Y thicknesses. For Gd/Pt/Co, on the other hand, the same authors [24] observed an oscillatory behaviour of the indirect exchange coupling through Pt layers. Suciu and co-workers [25] report a crossover of the bilinear and biquadratic couplings at a certain Cr thickness in Gd/Cr/Co multilayers. While these studies rely on macroscopic magnetization measurements, hence can hardly explore the spin polarization of the spacer metal, Ohkochi *et al* [26] recently observed XMCD spectra from Gd/Cu multilayers at the Cu K and L edges. The K-edge XMCD probes the Cu magnetism via the $1s \rightarrow 4p$ electric dipole transition of the core electrons. Signals as large as $\pm 3 \times 10^{-3}$ in $\Delta\mu_K/\mu_{jump}$ were observed from a [Gd (5.46 nm)/Cu (1.8 nm)]$_{30}$ sample at 20 K, which is one order of magnitude larger than those from Co/Cu multilayers at room temperature [4]. This shows a significant orbital polarization of Cu electrons sandwiched between ferromagnetic Gd. A finite spin moment has been obtained from the L_{23} XMCD measurements of Ohkochi *et al* [26]. Here $\Delta\mu_K$ is the difference of the linear K-edge absorption coefficients for the two circular polarization states of probing x-rays and μ_{jump} is the jump height in μ_K at the absorption edge. A salient feature of the dichroic spectra observed by Ohkochi *et al* at the Cu K edge is the remarkable oscillations, showing negative and positive peaks at $E - E_0 \approx 1$, 7, 13 eV and 4, 10, 15 eV, respectively, where E_0 is the Cu K-edge energy (8979 eV) [26]. The quasi-periodic features, being virtually independent of temperature below the Curie temperature, $\sim$120 K in the [Gd(5.46 nm)/Cu(1.8 nm)]$_{30}$ multilayer, as well as of the applied in-plane field, should reflect the properties of spin-polarized Cu 4p states. Ohkochi *et al* attempted to explain the oscillatory XMCD profile in terms of a differentiated nonmagnetic absorption spectrum assuming *a priori* a small exchange splitting of the Cu 4p bands.

In this paper, we put forward a more proper account of the XAS (x-ray absorption spectroscopy) and XMCD spectra for multilayered Gd/Cu with the use of the fully relativistic Korringa–Kohn–Rostoker (KKR) formalism including spin–orbit interaction. The paper is

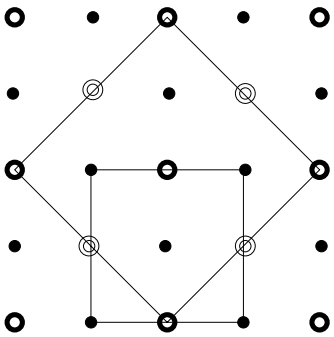

Figure 1. Model fcc Gd/Cu(001) structure. Large full circle, Gd layer 1; large open circle, Gd layer 2; small full circle, Cu layer 1; small open circle, Cu layer 2. The fcc Gd lattice is rotated by 45° around the [001] axis to match the fcc Cu lattice.

organized as follows. Section 2 presents the structure model used in our calculation, along with a brief description of the practical calculation procedure. The results are compared with the experimental spectra of Ohkochi *et al* in section 3. The calculation shows small but finite magnetic moments extended deep into the Cu layers. This leads us to propose in section 4 the hybridization of the Cu 4p states with the exchange-split Gd 5d states as the origin of Cu K-edge dichroism in multilayered Gd/Cu.

2. Structure model and theoretical approach

The samples investigated by Ohkochi *et al* include $[\mathrm{Gd}(5.46\,\mathrm{nm})/\mathrm{Cu}(1.8\,\mathrm{nm})]_{30}$ and $[\mathrm{Gd}(5.5\,\mathrm{nm})/\mathrm{Cu}(2.65\,\mathrm{nm})]_{15}$ multilayers, grown on polyimide films [26]. Wide-angle x-ray diffractometer scans show no discernible Cu peak, indicating a poor crystalline quality. To model this structure, we employ a close-packed fcc Gd(001)/Cu(001) structure with the fcc Gd lattice rotated by 45° around the [001] axis with respect to the Cu lattice (figure 1). The rotation allows the Gd lattice to match the fcc Cu lattice because bulk hcp Gd has a lattice parameter approximately $\sqrt{2}$ times as large as a_{Cu}. We assume that the model structure has the lattice parameter of bulk Cu ($a = 0.3615$ nm). In this model, Gd(5.46 nm)/Cu(1.8 nm) corresponds to Gd(21 AL)/Cu(10 AL), where AL stands for the (001) atomic layer. We performed, however, all our calculations on Gd(9 AL)/Cu(n AL) ($n = 1, 2, \ldots, 11$) in place of Gd(21 AL)/Cu(10 AL). This is because Gd(21 AL)/Cu(10 AL) is computationally more laborious and because we found that the central Gd layer (Gd_5) in Gd(9 AL)/Cu(n AL) already has bulk-like magnetic and electronic properties.

To calculate the electronic structure of multilayered fcc Gd/Cu(001), we employ the fully relativistic version of the KKR method [27]. This formalism allows the spin polarization and the spin–orbit coupling to be treated on the same level, enabling a proper calculation of XMCDs [28]. We treated exchange and correlation effects within the framework of local density functional theory, using the parametrization technique by Vosko *et al* [29]. As a first step of the *ab initio* calculations, we created the potentials self-consistently for Gd(9 AL)/Cu(n AL)(001) ($n = 1, 3, \ldots, 11$) multilayers using the atomic sphere approximation; the Wigner–Seitz cells are replaced by spheres of the same volume as a unit cell. We used Wigner–Seitz radii of 0.198 nm for Gd and 0.198 nm for Cu. In order to determine self-consistent potentials, we used a minimal 1000 **k**-points in the irreducible wedge of the Brillouin zone. These potentials are used in the calculations of the electronic and spectroscopic properties of the systems. The XMCD effects observed in x-ray absorption can be described straightforwardly within the framework of the KKR formalism (for review see [28]). For the calculations of the x-ray absorption coefficients μ the expression based on the Fermi's golden rule was used. Within this approach, the initial states are atomic-like core states belonging to the selected atom

Table 1. Calculated layer- and orbital-resolved valence electron numbers for the Gd(9 AL)/Cu (7 AL) (001) multilayer. Charges for Cu2 and Cu4 correspond to the averaged value of two chemically inequivalent sites in the second and fourth layers.

Gd(9 AL)/Cu(7 AL) (Charge/atom)	Gd					Cu			
	Gd_5	Gd_4	Gd_3	Gd_2	Gd_1	Cu_1	Cu_2	Cu_3	Cu_4
6s	0.736	0.736	0.741	0.741	0.745				
4s						0.734	0.713	0.699	0.707
6p	0.448	0.451	0.455	0.426	0.579				
4p						0.656	0.766	0.753	0.733
5d	1.479	1.481	1.487	1.418	1.446				
3d						9.522	9.553	9.537	9.539
4f	7.334	7.332	7.336	7.325	7.428				
Total	9.998	9.999	10.019	9.909	10.198	10.912	11.032	10.989	11.01

Table 2. Layer-resolved spin (μ_s) and orbital (μ_l) magnetic moments calculated for the Cu (7 AL)/Gd(9 AL) (001) multilayer. Spin and orbital moments for Cu_2, Cu_4 are the mean values for two chemically inequivalent sites in the second and fourth layers.

Gd(9 AL)/Cu(7 AL) (μ_B/atom)	Gd					Cu			
	Gd_5	Gd_4	Gd_3	Gd_2	Gd_1	Cu_1	Cu_2	Cu_3	Cu_4
μ_s	7.116	7.125	7.139	7.193	7.023	0.0196	−0.0041	−0.0039	−0.0036
μ_l	0.604	0.593	0.603	0.639	0.496	0.0001	−0.0000	−0.0001	−0.0000

absorption edge. Unoccupied final states are represented by the one-electron Green function evaluated within the framework of multiple scattering KKR theory. In contrast to the other calculation schemes, the resulting expression for the absorption coefficient is quite general and is even applicable to systems which do not have three-dimensional translational invariance, such as disordered alloys or surface systems.

3. Calculated spectra and comparison with observations

3.1. Electronic and magnetic structures

Table 1 shows the layer- and orbital-resolved valence electron configurations calculated for the $[Gd(9\ AL)/Cu(7\ AL)(001)]_{30}$ multilayer. The valence charges oscillate slightly in both the Cu and Gd layers. It is seen that 1.39, 1.48, 1.45, and 1.44 4s + 4p electrons are located on Cu_1, Cu_2, Cu_3, and Cu_4, respectively (index $_1$ corresponds to the interface layers). Note that 0.1 4p electron is transferred from Cu_1 to the 6p state on Gd_1. Away from the interface into the Gd layer, the electron configuration is already bulk-like on Gd_2. Table 2 shows the element- and layer-resolved spin (μ_s) and orbital (μ_l) magnetic moments calculated for the Gd(9 AL)/Cu(7 AL)(001) multilayer. These moments have been calculated in the direction perpendicular to the interface. Compared with our theoretical bulk value ($\mu_s = 7.14\ \mu_B$), the calculated Gd spin moment is slightly smaller on the interface layer (Gd_1), while larger on the second layer (Gd_2). A near-bulk value of $\mu_s = 7.12\ \mu_B$ is found on the core layer (Gd_5). We see the same trend in the orbital moments ($\mu_l = 0.56\ \mu_B$ for bulk Gd). While spin-magnetic moment stems mostly from the unpaired 4f electrons in Gd, the near-bulk spin and orbital moments obtained demonstrate the accuracy of our calculation.

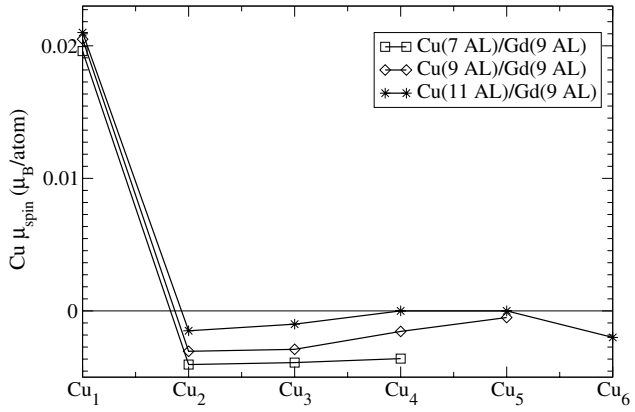

Figure 2. Calculated layer-resolved spin magnetic moments of Cu in the Gd(9 AL)/Cu(n AL) (n = 7, 9, 11) structures.

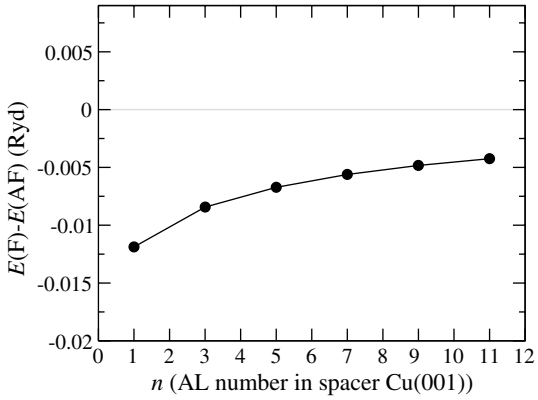

Figure 3. Interlayer exchange coupling energy calculated for Gd(9 AL)/Cu(n AL) (n = 1, 2, . . . , 11) multilayers.

For Cu, we find small spin and orbital moments of $\mu_s = 0.02\ \mu_B$ and $\mu_l = 0.0001\ \mu_B$ on the interfacial Cu site (Cu_1), which decrease towards the core of the Cu layer. Surprisingly, neither the spin nor the orbital moments vanish on the central layer (Cu_4). This size effect is more clearly seen in figure 2, where we show the layer-resolved Cu spin moments calculated for $n = 7, 9$ and 11 in the Gd(9 AL)/Cu(n AL) multilayer. As n decreases, the Cu electrons are more strongly magnetized in the near-interface layers and the polarization penetrates deeper into the Cu layer. The extended Cu magnetization is in line with the experimental inference by Ohkochi *et al* [26], but is in contrast to the rapidly decaying moments in Co/Cu calculated by Wu and Freeman [30] and Samant *et al* [11]. Hirai's calculation for Fe/Cu [31] shows a similar rapidly decaying Cu magnetization. We will come back to this point in a later section of this paper.

Figure 3 shows the interlayer coupling energy calculated for the Gd(9 AL)/Cu(n AL) ($n = 1, 2, \ldots, 11$) systems as a function of the spacer-layer thickness n. The interlayer coupling energy is the difference of the total energy between the parallel (F) and anti-parallel (AF) alignments of the Gd moments. A straightforward calculation requires the fully relativistic self-consistent calculation of the total energies for the two alignments, which is a very demanding computational task. Instead, we used the so-called force theorem method [30]. In this approach, only the band energies, e.g. the sum of the single-particle energies below the Fermi level, have to be calculated and not the total energy. The self-consistent spin-polarized relativistic calculation is performed only for parallel (F) configuration. Based on this self-consistent potential, a few iterations were carried out for the anti-parallel (AF) configuration

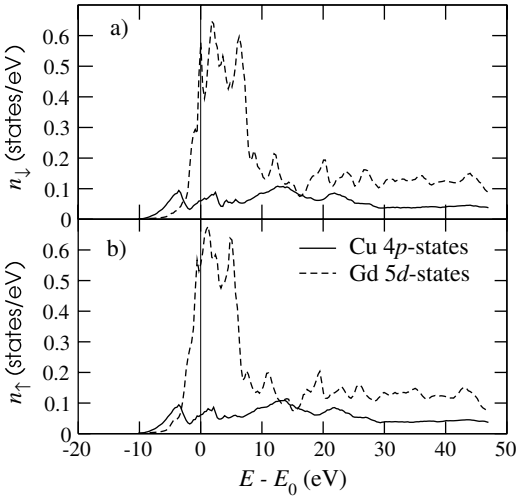

Figure 4. Spin-resolved density of states for the Gd 5d states and the Cu 4p states.

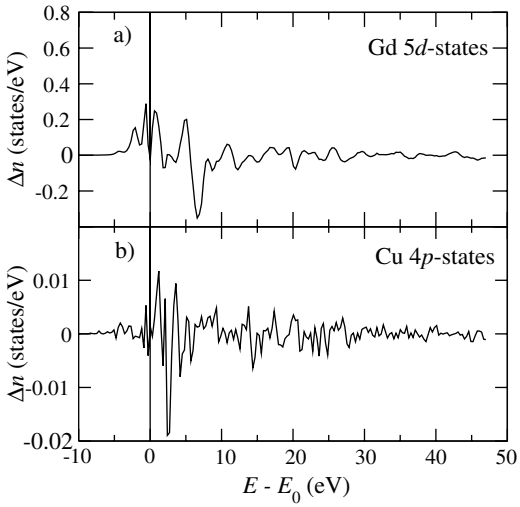

Figure 5. Difference density of states or spin asymmetry, Δn $(= n_\uparrow - n_\downarrow)$, for the Gd 5d states and the Cu 4p states.

in order to find a new Fermi level and to ensure the charge neutrality. In order to prove the validity of this approach, we performed self-consistent fully relativistic calculations for one of the systems, deducing the interlayer exchange coupling energy from the total energy. We found a very good agreement with results based on the force theorem. Figure 3 shows the band-energy difference $E(\mathrm{F}) - E(\mathrm{AF})$ per atom. For all Gd(9 AL)/Cu(n AL) systems studied, we find the parallel (F) alignment to be more stable. This makes a contrast to the oscillatory behaviours well known in the 3d, 4d, 5d metal/Cu systems. On the other hand, our theoretical results do not contradict Ohkochi *et al* [26], who report the absence of strong interlayer exchange coupling in their multilayers.

X-ray absorption measurements at the Cu K edge probe unoccupied 4p states above the Fermi level, even though a small contribution should come from the 1s $\rightarrow$ 3d quadrupole transition. In figure 4, we show the spin-resolved densities of states (DOSs) $n(E)$ for the Cu 4p states calculated using the KKR formalism, along with those for the Gd 5d states. The small exchange splitting of the Cu $4p_\uparrow$ and $4p_\downarrow$ bands is more clearly seen in figure 5, where

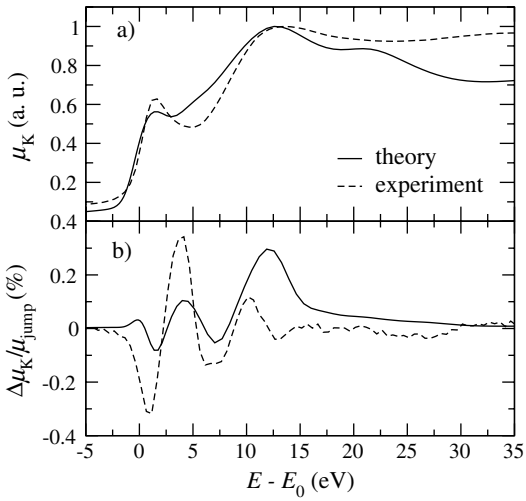

Figure 6. Theoretical (full line) and experimental (broken line) Cu K-edge XAS (upper panel) and XMCD (lower panel) spectra for the $[Gd/Cu]_{30}$ (001) multilayer. The experimental spectra are for the $[Gd(5.46\ nm)/Cu(1.8\ nm)]_{30}$ quoted from Ohkochi *et al* [26].

we show the difference DOS, Δn, defined by $n_\uparrow(E) - n_\downarrow(E)$. The exchange splitting of the Cu 4p states can be ascribed to the hybridization with the Gd 5d states, as can be seen from the corresponding splitting of the Gd $5d_\uparrow$ and $5d_\downarrow$ states. Interestingly, switching off the effective magnetic moments induced on the Cu sites, by averaging of the spin-up and spin-down Cu potentials, affects the exchange splitting of the Cu 4p states only marginally. Similar effects have been found in Co/Pt multilayers by Uba *et al* [32, 33]. These authors manipulate the effective moments on the Pt sites to find little effects on the magneto-optical properties.

3.2. XMCD spectra at the Cu K edge

We show in figure 6 the theoretical nonmagnetic (XAS) and dichroic (XMCD) absorption spectra near the Cu K edge calculated for the Gd(9 AL)/Cu(7 AL)(001) structure. The quadrupole transitions are weak at the K edges of Cu because the 3d shell is almost full. Therefore we used here the dipole approximation to calculate absorption coefficients. The broken line shows the experimental spectra for the $[Gd(5.46\ nm)/Cu(1.8\ nm)]_{30}$ multilayer at 20 K, taken from Ohkochi *et al* [26]. To make a direct comparison feasible, we convoluted the theoretical spectra with a Lorentzian of 0.2 eV in full width at half maximum (FWHM), accounting for the finite core-hole lifetime, and with a Gaussian of 0.4 eV in FHWM, representing the experimental resolution. A good overall agreement is seen in the XAS spectra in the near-edge region up to $E - E_0 \approx 20$ eV, beyond which the calculated $\mu_K(E)$ deviates from the observed one (figure 6(a)). The calculation shows a less enhanced prepeak at $E \approx E_0$, compared with the observation. Because the $1s \rightarrow 4p$ dipole transition dominates the absorption process, $\mu_K(E)$ reflects primarily the density of states of unoccupied 4p-like states above the Fermi level. No strict correspondence is seen, however, between $\mu_K(E)$ and the difference density of states shown in figure 5. This can be ascribed to the energy dependence of the transition matrix elements as well as to the broadening mechanisms used here (see above) [34].

The calculation reproduces the pronounced oscillatory behaviour of the Cu K-edge dichroism in the near-edge region, even though the signal level is as low as 0.3% or less in $\Delta\mu_K/\mu_{jump}$ (figure 6(b)). The agreement with the observed profile is, however, less satisfactory than in the XAS spectra. The calculated XMCD spectrum shows the first positive peak and the second negative peak at the correct energies ($E - E_0 \approx 4$ and 7 eV, respectively), but there are significant discrepancies between the theoretical and experimental energies of the first

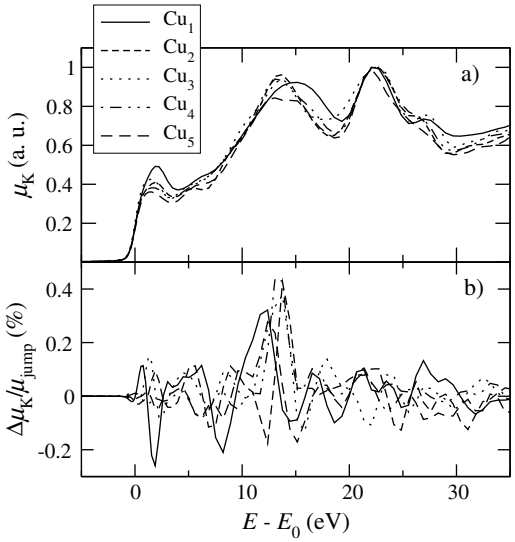

Figure 7. Layer-resolved XAS (upper panel) and XMCD (lower panel) spectra calculated for the [Gd(9 AL nm)/Cu(7 AL)$_{30}$ (001) multilayer at the Cu K edge.

negative peak ($E - E_0 \approx 1$ eV) and the second positive peak ($E - E_0 \approx 10$ eV). In addition, the calculation largely underestimates the modulation amplitudes below $E - E_0 \approx 10$ eV, while it overestimates at higher energies. The calculation shows a small positive peak at $E \approx E_0$, which is missing in the observed profile. These disagreements can be traced back to the structure model indicated in figure 1. The K-edge spectra are known to be highly sensitive to the structure of the system. In a later section of this paper, we will discuss the validity of the local density approximation used in our calculation.

As indicated in table 2 and figure 2, the induced magnetic moments at the Cu sites are largest on the interface Cu layers, but small more or less constant moments are observed on all other sites. This suggests that all Cu layers make finite contributions to the dichroic spectrum. This is indeed confirmed in figure 7, where we show the layer-resolved Cu K-edge XMCD spectra calculated for the Gd(9 AL)/Cu(7 AL)(001) structure. While the interfacial Cu layer, Cu$_1$, dominates in the near-edge region, all layers make comparable contributions at $E - E_0 > 12$ eV.

4. Discussion

A possible origin of the disagreements between the theoretical and experimental XCMD spectra can reside in the density functional theory used in our calculation. We assumed that core holes only broaden absorption profiles, without affecting the band structure for the final states. In reality, when an electron is photo-excited, a core hole is created and the final states change. As was demonstrated by Schwitalla and Ebert [35], based on the time-dependent density-functional theory, this effect can be accounted for in a very satisfying way by solving the corresponding Bethe–Salpeter type of equation for absorption coefficient. While this is beyond the scope of this paper, such an approach would not append much information because we do not expect a substantial change in the dichroic spectrum [36]. Another possible simple approach to the electron–hole interaction is to use, for the description of the excited state, energies and orbitals from a system where the absorber atom has a hole in the core level (final-state approximation [37]). However, by using this approach we did not find a significant change in calculated Cu XMCD K-edge spectra.

It is likely that the discrepant calculated spectra are affected by the cut-off of the orbital momentum expansion at $l = 4$ in our calculation. Calculations beyond $l = 4$ would improve the agreement of calculated XAS spectra with the observation in their high-energy part because the free-electron-like states high above the Fermi level are more appropriately described. However, such an approach would lead to a sizable increase of the computer time. By increasing l by one, computer time for the calculations of wavefunctions and inversion of the KKR matrix would double. Therefore, we performed corresponding orbital momentum convergence tests only on the smaller CuGd system of the CsCl structure. The XAS and XMCD spectra slightly changed by increasing the l-expansion, but one can say that at $l = 4$ the spectra are converged. We accept similar behaviour for the multilayer system investigated here.

We are convinced that the main cause of the disagreements with experiment at high energies in the XMCD spectra is related to the structure model used in the calculation, which oversimplifies the amorphous-like sample structures. In figure 7, all Cu layers show oscillatory behaviours with more or less similar amplitudes. A main difference between the individual layers is seen in the energy range of $E - E_0 = 10$–20 eV, where Cu_1 interface atoms show a broad positive peak at $E - E_0 \approx 10$ eV, while Cu_2 atoms show negative and positive peaks. An amorphous sample involves many inequivalent Cu atoms. Summing up the contributions from these sites can result in XMCD spectra in disagreement with those calculated for a simple single-crystal model.

We give below a simplified account for the origin of the Cu K-edge dichroism observed in Gd/Cu multilayers. Because of the extremely small exchange splitting of the initial 1s core states, it is apparently the exchange split and spin–orbit coupling of the final 4p states that is responsible for the Cu dichroism. The spin–orbit coupling of the 4p states causes an effective spin polarization on excited core electrons. For a circular dichroism to be produced, we need spin asymmetry in addition. This asymmetry is generated primarily by the hybridization of the Cu 4p states with the exchange-split Gd 5d states. The small but finite spin moments on the Cu sites far from the interface suggest that the strongly localized Gd 4f states do not directly polarize Cu atoms. This means that even if Cu has no induced magnetic moment, the Cu 4p–Gd 5d hybridization effectively splits the spin-up and spin-down Cu 4p states. This can be checked by turning off the induced magnetic moments on the Cu sites, which has actually led to very small changes in the Cu dichroism. A similar marginal contribution of Cu magnetic moments to XMCD has been confirmed in the Co/Cu system by the multiple-scattering calculation [4]. Turning off the spin–orbit coupling on the Gd site, on the other hand, resulted in a very small dichroism. As Igarashi and Hirai [38] show, the spin–orbit coupling of the Gd d states plays a role in generating the XMCD from Cu. These authors suggest that the d-orbital moments of nearby Fe sites induce the p-orbital moments on the x-ray absorbing Cu sites through the p–d hybridization.

Finally, we comment on the different Cu polarization behaviours in 3d/Cu and 4f/Cu multilayers. In Co/Cu and Fe/Cu multilayers, hybridizations take place between the Cu 4p and the (Co, Fe) 3d states. The calculations show no spin or orbital moments on the core-layer Cu in Co/Cu and Fe/Cu (see Wu and Freeman [30] and Samant *et al* [11]), even though the Co 3d and the Fe 3d states are strongly polarized. The Gd 5d polarization is quite weak in comparison since it is induced by the 4f polarization. The Gd 5d states are much more delocalized, however, than the 3d states of Fe and Co because the 5d radial wavefunction has a greatly increased number of nodes. We believe that the Cu 4p–Gd 5d hybridization is the principal cause of the small but finite magnetic moments on Cu planes far from the interface. The quantum-well states may make some contribution even though we find no evidence for interlayer exchange coupling in this system.

Acknowledgment

This work was funded by the German BMBF (Bundesministerium für Bildung und Forschung) under contract FKZ 05 KS1WMB/1.

References

[1] Greg J F 2001 *Spin Electronics* (*Springer Lecture Notes in Physics* vol 569) ed M Ziese and M J Thornton (Berlin: Springer) p 3
[2] Parkin S S P 1991 *Phys. Rev. Lett.* **67** 3598
[3] For review see Himpsel F J, Ortega J E, Mankey G J and Willis E 1998 *Adv. Phys.* **47** 511
[4] Nagamatsu S, Matsumoto H, Fujikawa T, Ishiji K and Hashizume H 2004 *Phys. Rev.* B **70** 174442
[5] Bruno P 1995 *Phys. Rev.* B **52** 411
[6] Bruno P and Chappert C 1991 *Phys. Rev. Lett.* **67** 1602
[7] Brookes N B, Chang Y and Johnson P D 1991 *Phys. Rev. Lett.* **67** 354
[8] Garrison K, Chang Y and Johnson P D 1993 *Phys. Rev. Lett.* **71** 2801
[9] Carbone C, Vesscovo E, Rader O, Gudat W and Eberhardt E 1991 *Phys. Rev. Lett.* **71** 2805
[10] Kawakami R K, Rotenberg E, Escocia-Aparicio E J, Choi H J, Wolfe J H, Smith N V and Qiu Z Q 1999 *Phys. Rev. Lett.* **82** 4098
Qiu Z Q and Smith N V 2002 *J. Phys.: Condens. Matter* **14** R169
[11] Samant M G, Stöhr J, Parkin S S P, Held G A, Hermesmeier B D, Herman F, Shilfgraarde M van, Duda L C, Mancini D C, Wassdahl N and Nakajima R 1994 *Phys. Rev. Lett.* **72** 1112
[12] Pizzini S, Fontaine A, Giorgetti C, Dartyge E, Bobo J-F, Piecuch M and Baudelet F 1995 *Phys. Rev. Lett.* **74** 1470
[13] Hayasaki Y, Ishiji K, Hashizume H, Hosoito N, Omote K, Kuribayashi M, Srajer G, Lang J C and Haskel D 2004 *J. Phys.: Condens. Matter* **16** 1915
[14] Parkin S S P, Bhadra R and Roche K P 1991 *Phys. Rev. Lett.* **66** 2152
[15] Johnson M T, Purcell S T, McGee N W, Coehoorn R, de Stegge J aan and Hoving W 1992 *Phys. Rev. Lett.* **68** 2688
[16] Bloemen P J H, Dalen R van, de Jonge W J M, Johnson M T and de Stegge J aan 1993 *J. Appl. Phys.* **73** 5972
[17] Bennett W R, Schwarzacher W and Egelhoff W F Jr 1990 *Phys. Rev. Lett.* **65** 3169
[18] Petroff F, Barthélemy A, Mosca D H, Lottis D K and Fert A 1991 *Phys. Rev.* B **44** 5355
[19] Fuß A, Demokritov S, Grünberg P and Zinn W 1992 *J. Magn. Magn. Mater.* **103** L221
[20] Unguris J, Celotta R J and Pierce D T 1994 *J. Appl. Phys.* **75** 6437
[21] Unguris J, Celotta R J and Pierce D T 1997 *Phys. Rev. Lett.* **79** 2734
[22] Okuno S N and Inomata K 1993 *Phys. Rev. Lett.* **70** 1711
[23] Takanashi K, Fujimori H and Kurosawa H 1993 *J. Magn. Magn. Mater.* **126** 242
[24] Takanashi K, Kurosawa H and Fujimori H 1993 *Appl. Phys. Lett.* **53** 1585
[25] Suciu G, Tousaint J C and Voiron J 2002 *J. Magn. Magn. Mater.* **240** 229
[26] Ohkochi T, Hosoito N, Mibu K and Hashizume H 2004 *J. Phys. Soc. Japan* **73** 1962
[27] Ebert H 2000 *Electronic Structure and Physical Properties of Solids* (*Springer Lecture Notes in Physics* vol 535) ed H Dreyssé (Berlin: Springer) p 191
[28] Ebert H 1996 *Rep. Prog. Phys.* **59** 1665
[29] Vosco S H, Will L and Nusair N 1980 *Can. J. Phys.* **58** 1200
[30] Wu R and Freeman A L 1996 *J. Appl. Phys.* **79** 6500
[31] Hirai K 2004 *Physica* B **345** 209
[32] Uba S, Uba L, Perlov A, Yaresko A N and Antonov V N 1997 *J. Phys.: Condens. Matter* **9** 447
[33] Uba S, Uba L, Yaresko A N, Perlov A, Antonov V N and Gontarz R 1998 *J. Phys.: Condens. Matter* **10** 3769
[34] Guo G Y, Ebert H and Temmerman W M 1991 *J. Phys.: Condens. Matter* **3** 8205
[35] Schwitalla J and Ebert H 1998 *Phys. Rev. Lett.* **80** 4586
[36] Ankudinov J, Nesvizhskii A I and Rehr J J 2003 *Phys. Rev.* B **67** 115120
[37] Brouder C, Alouani M and Bennemann K H 1996 *Phys. Rev.* B **54** 7334
[38] Igarashi J and Hirai K 1994 *Phys. Rev.* B **50** 17820